Proceedings of ASME Turbo Expo 2017: Turbine Technical Conference and Exposition
GT2017
June 26-30, 2017, Charlotte, NC, USA

GT2017-64285

DEMONSTRATION OF A DYNAMIC CLEARANCE SEAL IN A ROTATING TEST FACILITY

Andrew Messenger[*], **Richard Williams**
Grant Ingram, **Simon Hogg**
School of Engineering and Computing Sciences
Durham University
Durham, UK, DH1 3LE

Stacie Tibos
Jon Seaton
Bernard Charnley
GE Power, Steam Power Systems
Rugby, UK, CV21 2NH

ABSTRACT

The successful demonstration of the "Aerostatic Seal" in a half scale rotating facility is described in this paper. The Aerostatic seal is a novel dynamic clearance seal specifically designed for steam turbine secondary gas path applications. The seal responds to radial rotor excursions, so a reduced clearance can be maintained compared to conventional labyrinth seal without damage to the seal. This enables increased turbine performance through reduced leakage and increased tolerance of turbine transient events typically found during start up. The seal is an extension of the existing retractable seal design already deployed in commercial steam turbines.

The seal was tested in the Durham Rotating Seals Rig, which was developed specifically to test this device. The rig featured a rotor designed to run with large eccentricities to model high speed radial rotor excursions, and the seal was instrumented to measure the real time seal response to the rotor.

The experimental campaign has conclusively demonstrated the ability of the seal to dynamically respond to the rotor position. The key result is that the seal is able to track the rotor position at high speed, and hence maintain a mean seal clearance that is lower than the rotor eccentricity. Overall this work marks a key milestone in the development of the Aerostatic Seal, and leads the way to testing in a steam environment and application in steam turbine plant.

NOMENCLATURE

c	Clearance [m]
D	Rotor diameter [m]
e	Rotor eccentricity (zero to peak) [m]
e/R	Eccentricity ratio [-]
$\dot{m}$	Mass flow rate [kg/s]
P	Static Pressure [Pa]
PR	Pressure ratio [-] $PR = \frac{P_{in}}{P_{out}}$
R	Rotor radius [m]
Re_x	Axial Reynolds Number [-] $Re_x = \frac{2\dot{m}}{\eta\pi D} = \frac{2\rho vc}{\eta}$
T	Static temperature [K]
Ta	Taylor Number [-] $Ta = \frac{2uc\rho}{\eta}\sqrt{\frac{2c}{D}}$
u	Rotor surface velocity [m/s]
v_x	Leakage axial velocity [m/s]
α	Circumferential angle [°]
η	Dynamic viscosity [kg/m s]
ΔT	Time shift [s]
μ_{stat}	Coefficient of static friction [-]
ρ	Fluid density [kg/m^3]
ω	Rotor rotational speed [rpm]
Subscripts	
in	Inlet Conditions
out	Outlet Conditions
0	Stagnation Condition
+ve	Positive
-ve	Negative

[*]Address all correspondence to this author.

INTRODUCTION

In recent years an increased level of intermittent generation on the electrical grid has resulted in the requirement for conventional generators to operate more flexibly to meet electrical demand and remain profitable. For a steam turbine, flexibility in operation requires faster load changes, in turn leading to frequent transient radial rotor excursions and thermal expansions. Seals can then become damaged, reducing turbine efficiency and output power. A dynamic seal, which is a seal that can respond to the position of the rotor surface, offers major advantages over the conventional labyrinth seal. Not only can they accommodate rotor excursions, but they can operate at lower clearance, reducing leakage and hence increasing turbine efficiency. The "Aerostatic Seal", shown in Fig. 1, is a dynamic seal concept that is tested in this paper.

The Aerostatic Seal is a development of the retractable seal used in steam turbines for a number of years. The seal is made up from a number of circumferential seal segments; each seal segment consists of a labyrinth seal with an enlarged central pocket supplied with fluid from immediately upstream of the seal [1]. This central pressurised pocket allows the seal segment to move away from the rotor when at low clearances preventing the seal contacting the rotor surface. At high clearances reduced pressure in the central pocket moves the seal towards the rotor surface. As in a retractable seal, the seal segments are held apart by springs which stop the seal contacting the rotor when the turbine is under no load, shown in Fig. 1. The seal segments are pushed against the contact face of the gland holder by the difference between upstream and downstream pressure, and to be able to move each segment has to overcome the frictional force between the holder and seal segment.

Previous published work on the Aerostatic Seal has proven the concept and demonstrated the capability of the seal to move away and towards the rotor surface. This was achieved in a non-rotating test facility using air instead of steam [2, 3]. The advance presented here is the validation of the Aerostatic Seal in a rotating seals rig that features an eccentric rotor allowing radial rotor transients to be simulated. The seal has been tested with the rotor in both a low and high eccentric rotor position and successful operation obtained. In the high eccentric rotor position the seal segments were able to track the rotor over the full range of rotor speeds tested, and maintained a seal clearance which was lower than the level of rotor eccentricity. This lower clearance equates to a significant leakage reduction of 35% over a comparable labyrinth seal. This work paves the way for further development of the Aerostatic Seal outside of the laboratory.

Background

The labyrinth seal has found application in steam turbines since the initial development of such machines by C. A. Parsons in the late 19th century [4]. Labyrinth seals remain popular to this day due to their simplicity and relative ease of manufacture. Labyrinth seals consist of a number of throttles, with energy dissipated by viscous effects in the cavities after each throttle, dropping the pressure in subsequent cavities. Labyrinth seals are available in different arrangements; the most common are "straight", "stepped" or "staggered". Stepped or staggered seals have lower leakage as the high velocity fluid jet flowing under the fins is not able to travel straight under the subsequent fins as in a straight labyrinth seal [5].

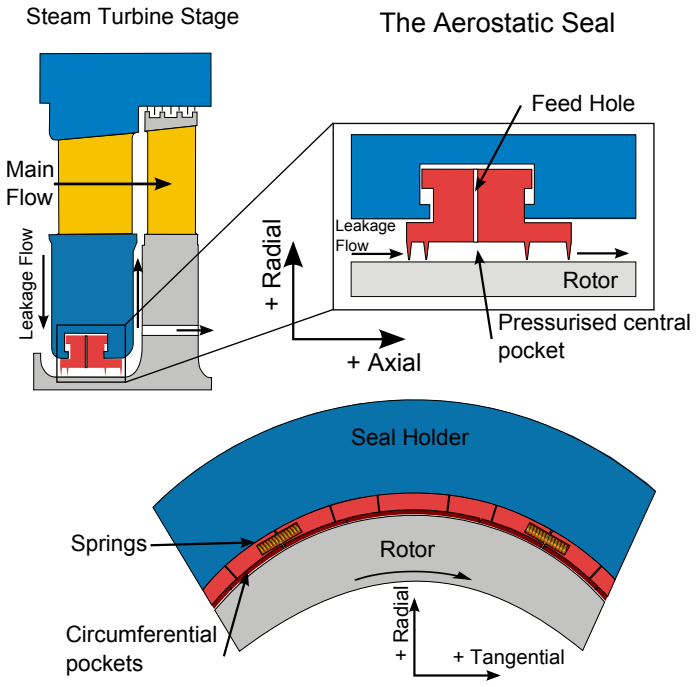

FIGURE 1. THE AEROSTATIC SEAL CONCEPT

The disadvantage of the labyrinth seal is the relatively high leakage flow rate through the seal and the intolerance to relative movement between the seal and the rotor surface, leading to seal damage and an increase in leakage flow [5]. Labyrinth seals also can introduce destabilising rotordynamic forces in steam turbines due to swirling flow inside the labyrinth seal cavities [6]. Swirl brakes at inlet to the seal can reduce the cross coupled stiffness of the seal, improving rotordynamic stability [7].

Attempts have been made to reduce the leakage flow rate through labyrinth seals. Many researchers have investigated geometric parameters of the labyrinth seal, such as fin pitch [8], tooth shape [9], cavity shape [10] and seal eccentricity [11] to name a few. The use of air curtains can also be utilised to improve the performance of labyrinth seals. Curtis et al [12] tested such a seal in a single stage turbine operating in air and demonstrated leakage reduction and overall efficiency gain. Hogg and Ruiz [13] used Computational Fluid Dynamics (CFD) simulations to pre-

dict the potential leakage reduction in a steam turbine, and found an improvement of 25% (including the air curtain flow) over a labyrinth seal operating at the same conditions.

The retractable labyrinth seal is another type of labyrinth seal [14]. The seal is divided into circumferential segments with springs that push the segments apart when the turbine is unloaded, creating a larger clearance between the labyrinth teeth and the rotor. This enlarged clearance is useful to prevent damage to the labyrinth fins due to increased rotor radial movement during start up. Once operating pressure has been reached the pressure force on the seal segment outer overcomes the spring force, reducing the seal clearance. The segments rest locked together at the designed clearance. If the rotor was to move radially towards the segments, there is no mechanism for the segments to increase clearance without rotor contact.

Brush seals are a more recent addition to steam turbine sealing. Brush seals consist of a dense pack of fine diameter wire bristles, sandwiched between an upstream and downstream plate, and welded on the outer diameter [5, 15]. The bristles are fitted such that they contact the rotor surface and are angled in the direction of the rotation of the rotor to prevent buckling. The advantages of the brush seal are a dramatic decrease in leakage flow (up to 80% [16]), reduction in required axial space and accommodation of shaft movements. Without careful design, brush seals can lead to localised heating of the rotor surface [5, 17].

Non-contacting dynamic seals have the potential to deliver similar levels of leakage reduction as brush seals without localised heating of the rotor and degradation of leakage performance over time. Currently dynamic seal technologies have yet to make their way into steam turbines, although they are under development for applications such as supercritical carbon dioxide (sCO2) Brayton cycles [18]. Two dynamic seal concepts published in the wider literature are discussed here; the "Hydrostatic Advanced Low-Leakage" (HALO) seal and annular floating ring seal. Both these seals utilise hydrodynamic and hydrostatic forces to avoid contact between the seal and the rotor.

The HALO seal is a dynamic seal that consists of cantilevered pads that are able to move radially. The pads are held by a radially soft but axially stiff spring, with a downstream secondary seal to prevent leakage through the spring section. Hydrodynamic and hydrostatic forces are used to control seal clearance [19]. The HALO seal has been tested in a high temperature seal test rig and a significant leakage reduction was achieved [20]. The HALO seal is commercially available.

Floating ring annular seals are dynamic seals that consists of a single annular ring made from carbon. For seal movement to occur, the seal ring has to overcome friction between itself and the stator, as in the Aerostatic Seal. The seal ring is made of carbon, and therefore the frictional forces acting on the seal ring are low. Including the effects of mixed lubrication, the equivalent coefficient of friction is expected to be below $\mu = 0.1$ [21]. The ability of the seal to track high speed and low amplitude rotor vibrations has been demonstrated in a rotating test facility [22].

The disadvantages of the HALO seal and floating ring annular seal for application to steam turbines are the complex manufacturing due to the requirement for close tolerances and new materials. Typical fluid film thickness in such seals are of the range 0.005-0.013 mm [18]. These seals would also require change to current steam turbine construction.

The Aerostatic Seal

The Aerostatic Seal offers advantages over other dynamic seal concepts as it is a development of currently used sealing technology in steam turbine seals. The addition of feed holes from the top surface of the seal segments to a central pocket allow the seal to respond to rotor movement. Due to the similarity of the design to existing diaphragm and end gland segments, the seal design can be retrofitted into existing diaphragm and end gland constructions.

The mechanism for the Aerostatic Seal to move radially is provided by the axial pressure distribution through the seal. Fig. 2 compares the axial pressure distribution at high and low clearance, the net radial force is produced by integrating the pressure over the axial length of the seal. The blue line represents the pressure acting on the top surface of the seal segment, and the red line the pressure acting on the bottom surface. At high seal segment clearances, the majority of the leakage flow is under the seal segment due to the large leakage area under the seal compared to the feed holes. Therefore the axial pressure distribution is similar to a conventional labyrinth seal, and due to inlet pressure acting on the top surface of the seal segment, there is a net radial force acting towards the rotor. At low clearances the flow rate through the feed holes is a significant proportion of the leakage flow, and as a consequence the pressure drop occurs at the final two restrictions. Through careful choice of geometry a force towards the rotor can be obtained at high clearances and a force away from the rotor obtained at low clearances. As in the retractable seal, circumferential springs are used which retract the seal segments when the pressure drop across the seal is low.

The pressure drop through the seal generates a net axial force, which is reacted by the seal holder. Due to metal-on-metal contact between the holder and the seal segments, a frictional force is generated. For the seal segment to move, the magnitude of the radial force must be greater than the frictional force.

All the forces acting on the seal segment generate a moment acting about the centroid of the seal segment, and which would cause the segment to tilt forward. This moment is balanced by the seal holder reaction force which acts on contact face and radially below the segment centroid, thus ensuring moment equilibrium. During the design phase, it is ensured that moment equilibrium is maintained at all operating clearances and pressures [2].

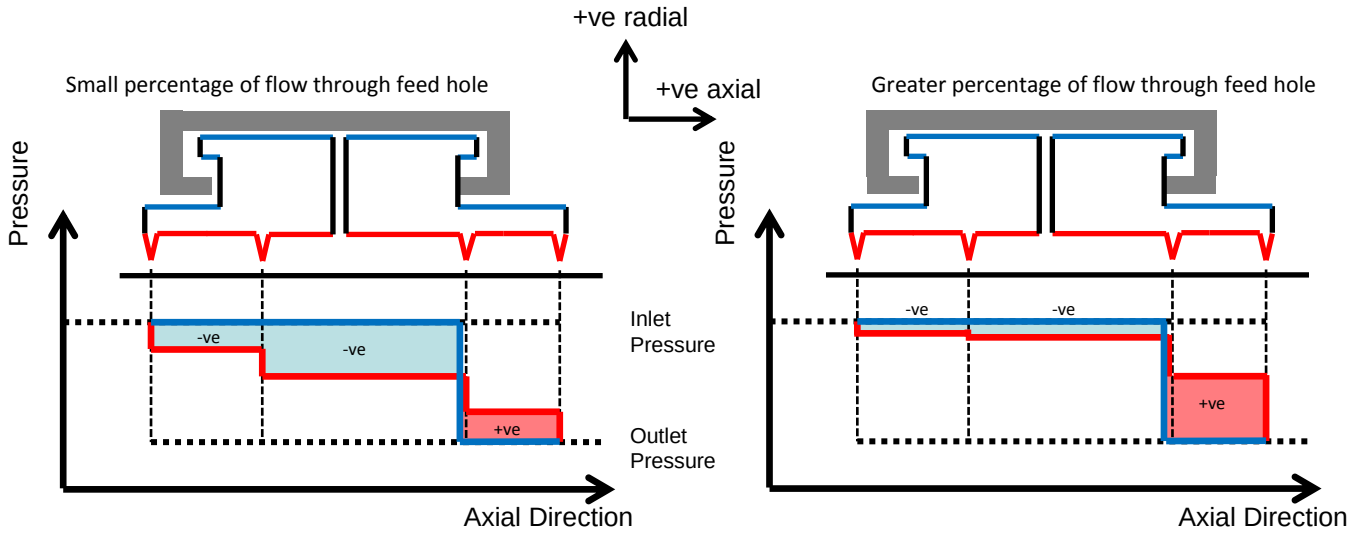

FIGURE 2. AXIAL PRESSURE DISTRIBUTION AT HIGH SEAL SEGMENT CLEARANCE (a) AND LOW SEAL SEGMENT CLEARANCE (b)

THE DURHAM ROTATING SEALS RIG

A rotating seals facility, the Durham Rotating Seals Rig, was designed and built to test the ability of the Aerostatic Seal to tolerate large transient radial rotor excursions at a range of rotor speeds. A cross section is shown in Fig. 3.

The facility consists of a rotor mounted on a cantilevered stub shaft, and is a 'single flow' arrangement. A pair of high capacity angular contact bearings resist the axial load due to the seal pressure difference and radial loads due to rotor eccentricity. The rotor is driven by a smaller inner shaft connected to the motor through a flexible coupling. The rotor has been manufactured as an inner rotor connected to the bearings and an outer rotor which can be positioned off centre to achieve rotor eccentricity. Although the two parts of the rotor are bolted together, two sets of pins are also included which consistently position the outer rotor section in a low eccentricity position (0.09 mm), or a high eccentricity position (0.55 mm). Eccentricity ratio has been defined as eccentricity divided by rotor radius (e/R) to aid comparison to different size of rotor and eccentricity levels, and is included in Tab. 1.

Inlet static pressure and temperature were measured, as well as the outlet static pressure and mass flow rate of air through the rig. There are six outlets from the rig to atmosphere, each one situated directly behind each seal segment. This allows the use of a camera to observe seal segment behaviour. Tab. 1 summarises the key facility parameters.

Air to the facility was supplied from a 10 m^3 receiver at 16.0 bar(a) pressure and room temperature, and the pressure regulated with a computer controlled valve. The facility was operated with an upstream bypass line to accommodate rapid pressure changes resulting from the changing clearances of the Aerostatic Seal.

TABLE 1. KEY FACILITY PARAMETERS

Rotor Diameter	D	0.366	m
Max. Inlet Pressure	P_{in}	6	bar (a)
Rotational Speed	ω	100-1500	rpm
High Eccentricity Setting	e	0.00055	m
High Eccentricity Ratio	e/R	0.003	-
Low Eccentricity Setting	e	0.00009	m
Low Eccentricity Ratio	e/R	0.0005	-
Surface Velocity at 1500 rpm	u	28.7	m/s
Max. Mass Flow Rate	$\dot{m}$	0.75	kg/s

The rotating facility had ten Keyence Ex-110 inductive displacement sensors to measure the seal segment positions: Six sensors were mounted around the periphery of the seal, and were used to measure the clearance between the rotor and the seal segments. In the configuration used in the testing described in this paper, all 6 sensors were used on the top 3 gland segments, 2 per segment. Two sensors measured the rotation of the top-dead-

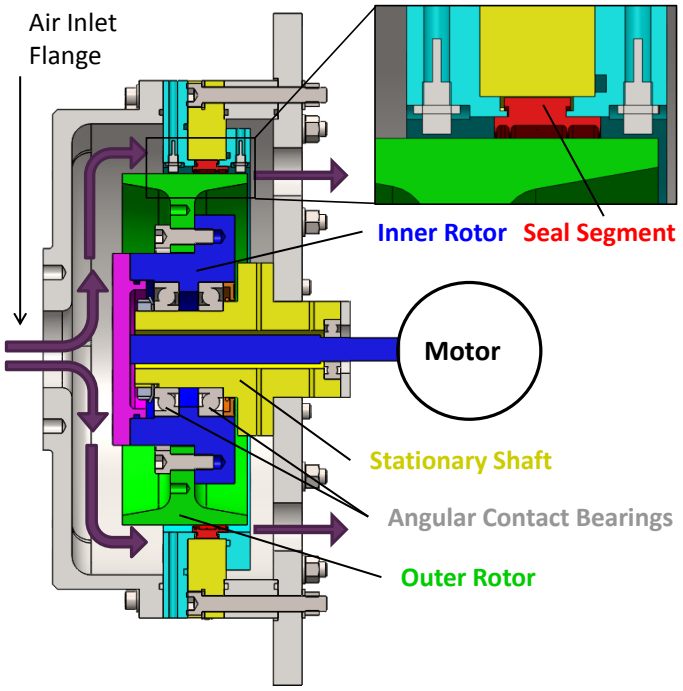

FIGURE 3. CROSS SECTION OF DURHAM ROTATING SEALS RIG

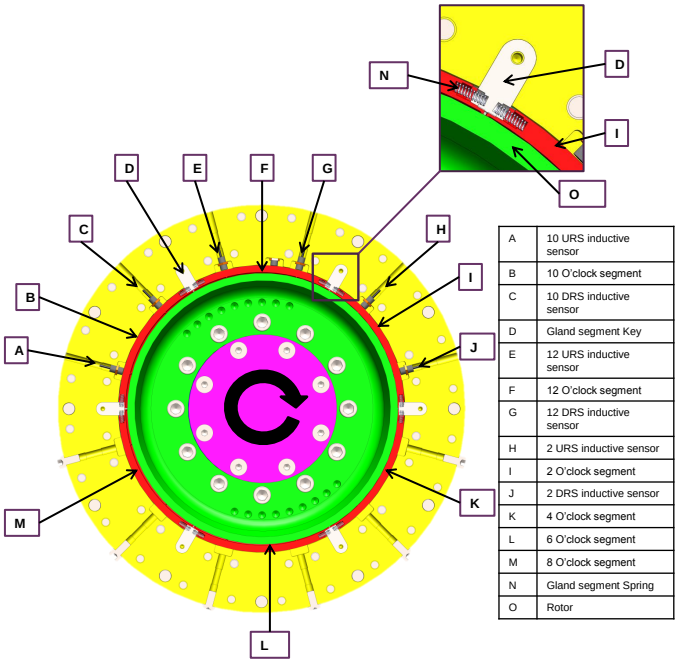

FIGURE 4. CIRCUMFERENTIAL SENSOR LOCATIONS

centre segment about the tangential axis. A further two sensors were used to measure the rotor position, measuring upstream and downstream of the top dead centre seal segment.

An analogy of a clock face is used when describing positions of seal segments and sensors, shown in Fig. 4, the rotor rotating in a clockwise manner. For example the top-dead-centre seal segment is designated the *12 O'clock segment*. Each seal segment on the top half of the rotor (10, 12 and 2 O'clock seal segment) was monitored by two inductive sensors, as shown in Fig. 4, and so the radial position of the seal segment is fully defined. Each sensor is referred to as either the up rotation side (URS) or down rotating side (DRS) sensor, with a point on the rotor surface moving from URS to DRS.

The seal segment inductive sensors were calibrated to give seal segment position relative to mean rotor surface position. The seal segment position sensors were not positioned at the same circumferential position as the rotor surface sensors. Therefore the seal segment position was time shifted by Eqn. 1 to reflect the different rotor position at different circumferential positions, where α is the relative circumferential angle between the rotor sensor and the seal segment sensor, ΔT is the time shift and ω is the rotor speed in rpm.

$$\Delta T = -\frac{\alpha}{36\omega} \tag{1}$$

TABLE 2. FACILITY INSTRUMENTATION AND CAPABILITY

Measurement		Range	Accuracy	Unit
Seal Clearance	c	0.00 to 2.00	0.00001	m
Inlet Pressure	P_{in}	0.00 to 17.24	±0.0086	bar
Outlet Pressure	P_{out}	0.00 to 6.89	±0.0035	bar
Tank Temperature	T_0	-100 to 400	±0.5	°C
Inlet Temperature	T_{in}	-200 to 1370	±0.5	°C
Seal Leakage	$\dot{m}$	0.05 to 0.25	0.001	kg/s
Rotor Speed	ω	60 to 1500	0.1	rpm

The rotating rig was equipped with an orifice plate to measure the leakage flow rate of air through the seal. Static pressure at inlet and outlet of the rig was measured at six points around the circumference of the inlet and outlet plenum. Pressure was measured using a ScaniValve DSA3217 16 channel pressure scanner with a maximum frequency of 800 Hz per channel. Inlet static temperature was also measured in the inlet plenum with a K type thermocouple and tank temperature with a T type thermocouple. Finally rotor rotational speed was measured with an opto sensor mounted above the motor coupling. Tab. 2 lists the instrumentation and capability.

AEROSTATIC SEAL DESIGN

Previous work on the Aerostatic Seal developed a design methodology [2]. This has been used to generate a seal design, designated 'ROT02', suitable for operation at test rig pressure conditions. The seal was made of 6 seal segments, each segment held circumferentially with springs and keys (shown in Fig. 4). The keys prevented the seal segments rotating with the rotor, and removed interdependence between different circumferential seal segments. The pressure ratio, defined by Eqn. 2, was used to non-dimensionalise the seal pressures at inlet and outlet of the seal. The design pressure ratio for ROT02 was chosen as $PR = 1.5$. Standard off the shelf springs were used in the design to enable seal segment retraction at low seal pressure differences. The seal segments and seal holder was made from S355J2G4 structural grade steel.

$$PR = \frac{P_{in}}{P_{out}} \tag{2}$$

One of the key parameters of Aerostatic Seal performance is the radial stiffness characteristic. This is the radial force acting on the individual seal segments over the operating clearance of the seal. The analytically predicted radial stiffness is shown in Fig. 5. The static friction present between the seal segment and holder creates a range of clearances at which the seal segment is unresponsive; this is the grey shaded region in Fig. 5. When designing the Aerostatic Seal, the coefficient of static friction was assumed to be $\mu_{stat} = 0.60$. This gave an unresponsive region between a clearance of 0.017 mm and 0.33 mm. If the coefficient of friction was greater, then the range of clearance at which the seal was unresponsive would be greater, as demonstrated in Fig. 5.

EXPERIMENTAL CAMPAIGN

Testing was conducted with the rotor in two positions: low eccentricity (0.09 mm) and high eccentricity (0.55 mm). The aim of the low eccentricity testing was to demonstrate Aerostatic Seal performance at similar levels of eccentricity found in a running turbine. High eccentricity testing was conducted to assess how responsive the Aerostatic Seal was to more extreme rotor radial transients, and to demonstrate the ability of the seal to move away from the rotor without metal on metal contact. A final set of tests were conducted with the seal segments fixed at a known position and the feed holes blocked. This provided an equivalent labyrinth seal to assess the leakage reduction of the Aerostatic Seal.

Low Eccentricity Tests

Initial testing was conducted with low rotor eccentricity and at rotor speeds of 0, 60, 600, 900 and 1500 rpm. Fig. 6 shows the seal segment mean clearance from a typical low eccentricity

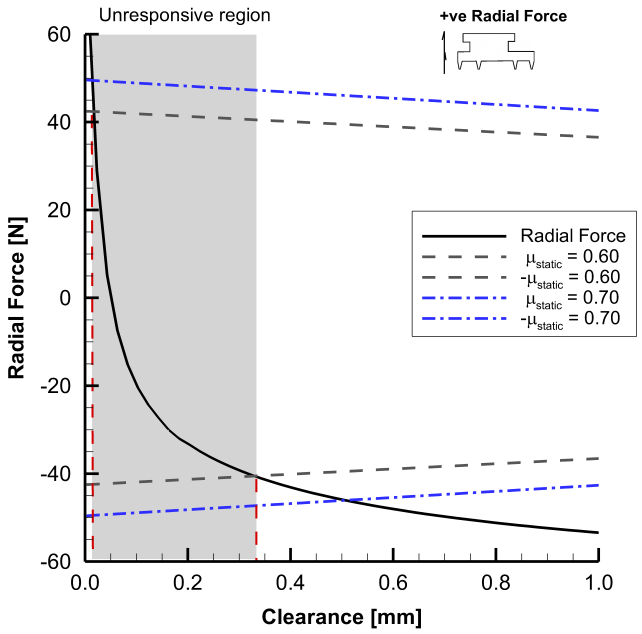

FIGURE 5. ANALYTICAL RADIAL STIFFNESS OF ROT02 SEAL DESIGN AT PRESSURE RATIO $PR = 1.5$

rotor test at a rotor speed of 1500 rpm. Results are presented for all three instrumented seal segments (10, 12 and 2 O'clock) and for both up rotation and down rotation sides of the segment. See Fig. 4 for nomenclature. From 0 to 5 seconds the seal segments were in the retracted position as there was only a small pressure difference across the seal. There was some variation in retracted seal segment clearance between seal segments and also between the URS and DRS of the 10 O'clock seal segment. This was due to the carrier ring which houses the seal segment being slightly off centre from the rotor and manufacturing tolerances between the keys which set the initial clearance.

The pressure ratio was increased, and once sufficient pressure ratio across the seal was achieved, at around 6 seconds, the seal segments moved towards the rotor surface. This happened quickly as once the seal segments started moving the friction force was reduced from static friction to dynamic friction. The seal segments then came to rest at the operating clearance where the mean clearance is not influenced by further increases in pressure ratio. At the operating clearance the difference in clearance between different sides of the seal segment was only around 0.05 mm.

As a consequence of the rotor eccentricity, the 12 O'clock seal segment was excited by the rotor, shown in Fig. 6, and enlarged in Fig. 7. After 11 s this excitation is damped out by the frictional force. Also of note is the difference in responsiveness

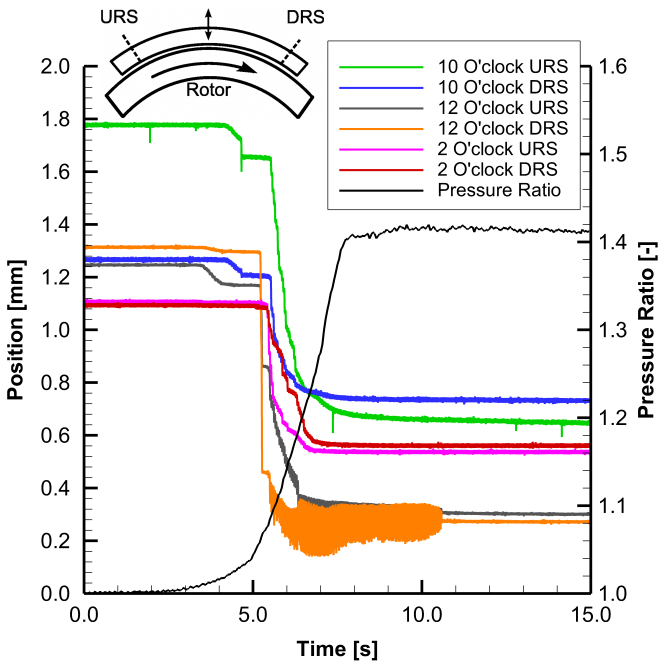

FIGURE 6. TYPICAL SEAL RESPONSE AT LOW ECCENTRICITY AND 1500 RPM

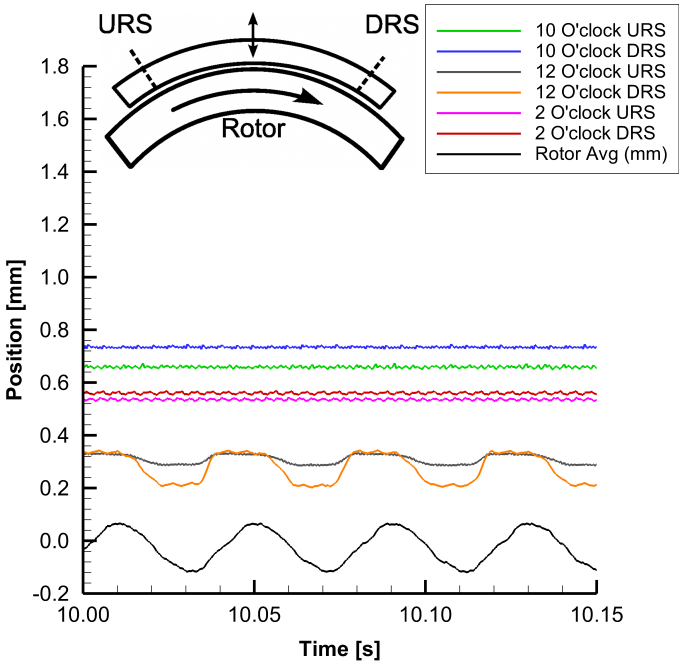

FIGURE 7. VIBRATORY RESPONSE AT LOW ECCENTRICITY AND 1500 RPM

of the URS and DRS sides of the seal segment. A similar effect was observed in a non-rotating test facility [3], and so is not due to the addition of shaft rotation. Although there appears to be a slight vibration on the other seal segments in Fig. 7; this was traced to a small oscillation of the output voltage from the amplifier circuitry of the inductive sensors, at approximately 800 Hz, and not related to the test.

The circumferential position of the seal segments was shown to have an effect on the response. The 12 O'clock segment was the first seal segment to move to the operating clearance. This was as expected since the gravitational force vector is entirely in the radial direction. The 10 and 2 O'clock segments moved later and at a higher pressure ratio, and maintained a slightly higher clearance than the 12 O'clock segment, due to the reduced radial component of gravitational force.

High Eccentricity Tests

A series of tests was conducted with high (0.55 mm) rotor eccentricity. The aim of the tests was to demonstrate the operation of the Aerostatic Seal to large and high speed rotor radial excursions. Testing was conducted at a range of rotor speeds: 100, 300, 600, 900, 1200 and 1500 rpm, and up to a maximum pressure ratio of $PR = 1.5$.

Fig. 8 plots the URS and DRS 12 O'clock seal segment position at a rotor speed of 1500 rpm and pressure ratio of $PR = 1.5$. The rotor position at both sensor locations has been plotted without the time shift correction applied. The seal segment was operating between a high and low position, and was stationary for a period of time at the high and low positions. Therefore before the seal segment could move, it had to overcome static friction rather than dynamic friction. There is a phase shift between the response of the seal segment and rotor positions of approximately 20°. Both sides of the seal segment move at the same time.

Fig. 9 plots the same results as Fig. 8 for the 10, 12 and 2 O'clock seal segments with the time shift correction applied to the seal segments. All seal segments had a similar response. Whilst only the top three seal segments were instrumented, a camera positioned at the outlet of the rig provided confirmation that all seal segments responded to the rotor. The 10 O'clock seal segment shows a greater difference in position between the URS and DRS of the segment; this was due to the uneven initial clearance, as found in Fig. 6.

Fig. 10 shows the mean clearance for each measured seal segment over the full range of rotor speeds and pressure ratios tested. The mean segment clearance has been obtained by numerically integrating the seal position with respect to time. Due to 0.55 mm eccentricity of the rotor, the minimum seal clearance that a fixed labyrinth seal could operate is 0.55 mm. This is also plotted in Fig. 10.

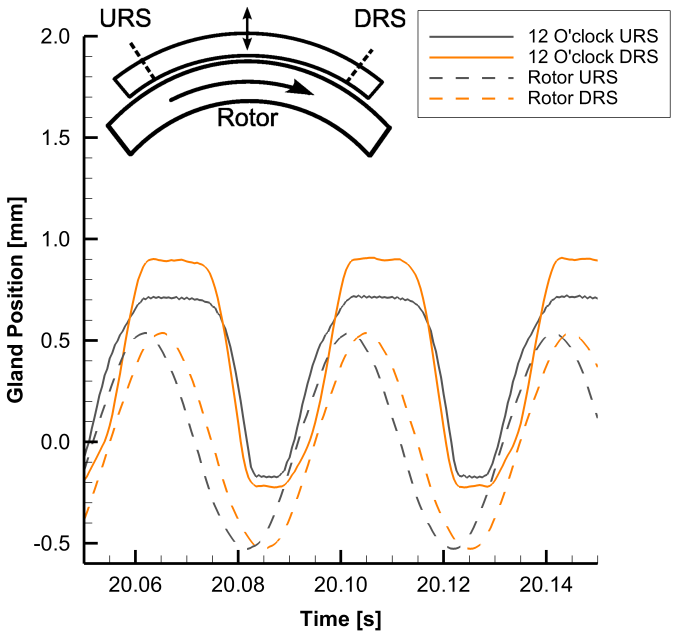

FIGURE 8. 12 O'CLOCK SEAL SEGMENT RESPONSE AT 1500 RPM WITH HIGH ECCENTRICITY

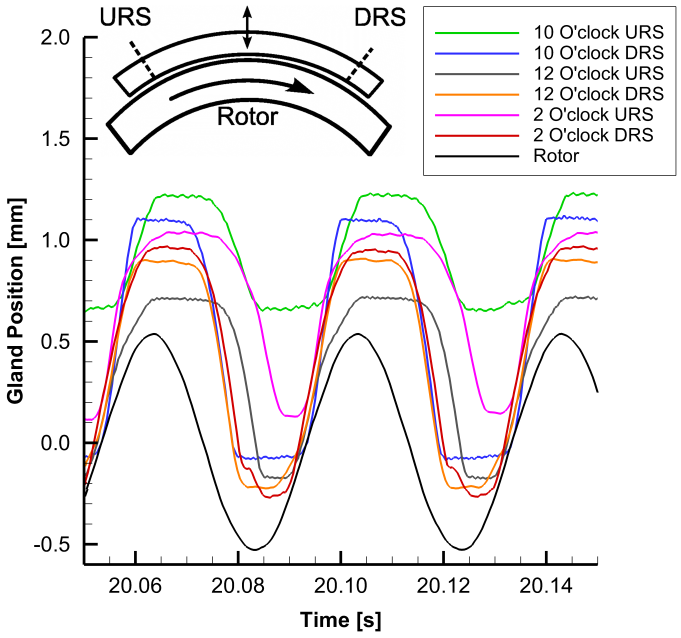

FIGURE 9. SEAL SEGMENT RESPONSE AT 1500 RPM WITH HIGH ECCENTRICITY

At a low pressure ratio of $PR = 1.1$ the influence of rotor speed was significant, particularly so for the 10 O'clock segment, and the seal was operating at a higher mean clearance. At a pressure ratio of $PR = 1.10$ the seal segments had only just moved from the retracted position, and the 10 O'clock segment was the last to move. However once the pressure ratio has increased to $PR = 1.15$ the effect of speed was reduced, and between pressure ratios of $1.3 < PR < 1.5$ the response is almost independent of rotor speed.

The key observation is that the seal segments were able to maintain a mean clearance that was lower than the level of rotor eccentricity once sufficient pressure ratio had been obtained. This is true over the full range of rotor speeds for the 12 and 2 O'clock seal segments. The 10 O'clock segment response was not as good, and demonstrates that initial position of the seal segment influences performance.

Potential Leakage Reduction

In order to assess the potential leakage reduction the Aerostatic Seal presents over a comparable labyrinth seal, the Aerostatic Seal segments were fixed in position with shims and the feed holes blocked with foil tape. The mean clearance of the whole seal, including the gaps between segments, was measured at 0.97 mm, and could tolerate 0.55 mm eccentricity of the rotor without contact. The gap between the seal segments was 4.9% of the total leakage area.

Leakage mass flow rate was measured with a low rotor eccentricity at a fixed rotor speed over a range of pressure ratios and shows a substantial reduction in leakage flow compared to the fixed clearance case, shown in Fig. 11. Leakage mass flow measurements with fixed seal clearance was taken over a range of rotor speeds from 600 to 1500 rpm, and there was no discernible difference in leakage mass flow rate. This was confirmed by considering the ratio of Taylor number (Ta) to axial Reynolds number (Re_x). Waschka et al [23] found no effect of rotational speed on seal discharge coefficient for $Ta/Re_x < 0.2$. The maximum ratio of Ta/Re_x for the tests conducted with fixed segments was approximately $Ta/Re_x = 0.03$.

Leakage mass flow rate was measured with high rotor eccentricity at various rotor speeds from 300 to 1500 rpm. The variation between data points is due to varying levels of friction between individual test runs, affecting the mean clearance of the gland segments and therefore leakage mass flow rate. The eccentric rotor data shows that the leakage through the seal was not significantly increased due to large radial rotor excursions. At the ROT02 seal design pressure ratio of $PR = 1.5$, an approximate 35% reduction in leakage mass flow was measured.

Analytical predictions for the fixed labyrinth seal were used to add confidence to the measurements taken with the fixed seal segments, and included in Fig. 11. Hodkinson's model [24], which uses Martin's leakage equation [25], with a coefficient of

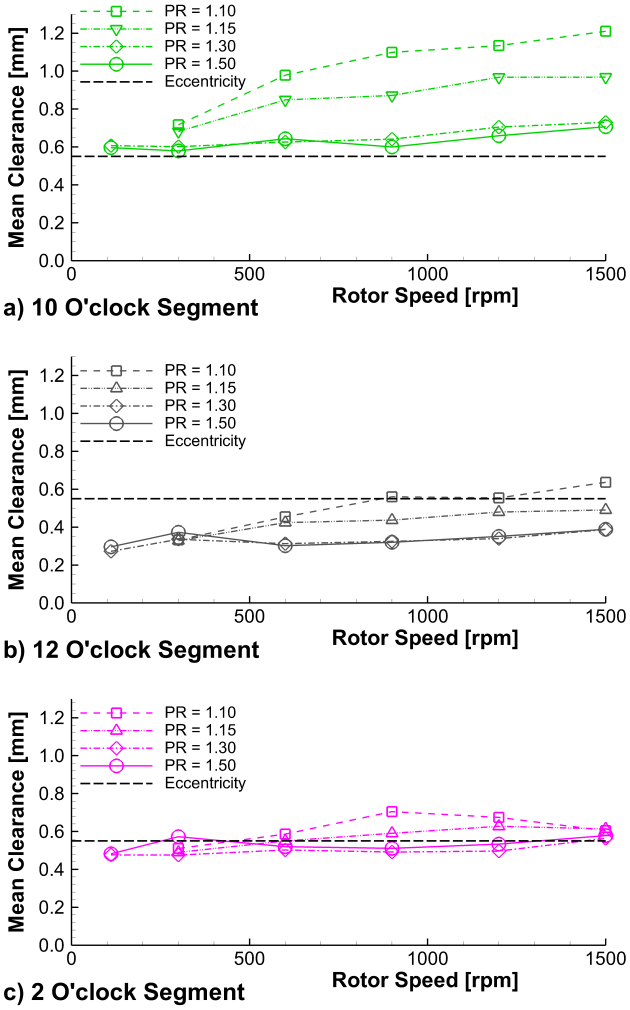

FIGURE 10. MEAN SEAL SEGMENT CLEARANCE WITH HIGH ECCENTRICITY

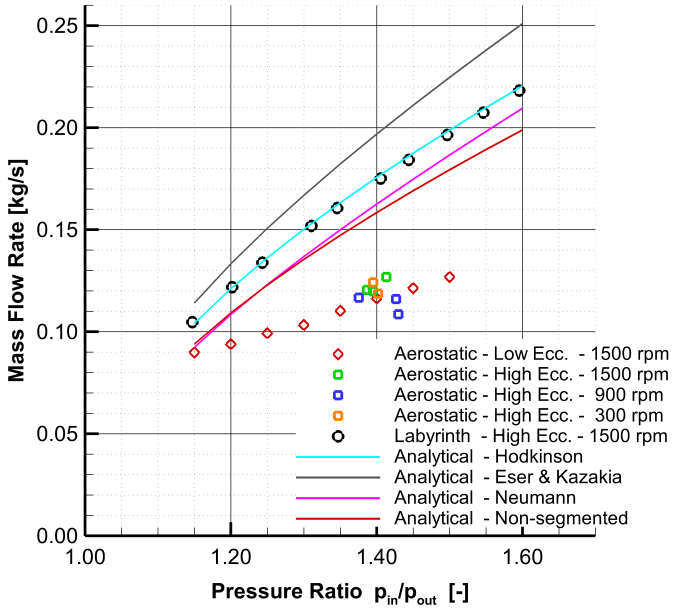

FIGURE 11. LEAKAGE MASS FLOW RATE

discharge $C_d = 0.60$ gave a good match to the fixed seal leakage data. The method of Neumann [6], which models the pressure drop across each labyrinth restriction and a pressure dependant coefficient of discharge based on ideal compressible flow theory derived by Chapygin [26], gave a reasonable leakage prediction, and captured the effect of pressure ratio on the leakage mass flow rate. Finally the method of Eser & Kazakia [27] was used, which is the leakage model used in the Aerostatic Seal analytical design tool. This method is reasonable at low pressure ratios but over predicts the mass flow rate at higher pressure ratios.

The analytical method of Hodkinson was used to obtain a comparison of the leakage through the Aerostatic Seal to a non-segmented labyrinth seal, and has been included in fig. 11. The leakage through a labyrinth seal is proportional to the leakage area, and inversely proportional to the square root of the number of restrictions [24]. As the gaps between the segments are a single restriction, and the labyrinth seal has four restrictions, then the leakage per area through the gaps is twice that of the main seal. Therefore if the gap area is 4.9% of the total leakage area of the seal, then 9.8% of the leakage flow rate is through the gaps. Comparing the measured leakage of the Aerostatic Seal to the predicted leakage through a non-segmented seal, the leakage benefit is still approximately 30% at the design pressure ratio of $PR = 1.5$.

DISCUSSION

The ideal operating characteristics of the Aerostatic Seal is to maintain a low clearance between the rotor and the seal. As there will inevitably be a small sub 0.1 mm run out on the rotor of a steam turbine, it is desirable that the seal segments do not respond to these small rotor movements to prevent excessive wear on the contact face. Only when there are large radial rotor excursions should the seal segments respond, or if thermal expansion reduced the seal clearance to an extent that there was a danger of the rotor contacting the seal.

Testing with the rotor in the low eccentricity position has demonstrated these desired operating characteristics of the Aerostatic Seal. The seal starts at a retracted position and moves to a low, static operating position. The low level of eccentricity was

able to excite the 12 O'clock seal segment, although this damped out after a few seconds. Seal segment circumferential location was shown to affect seal performance due to differing levels of gravitational force acting on the segment. At higher pressures the effect of gravity will be less significant due to increased pressure forces.

Testing conducted with high rotor eccentricity and speed has demonstrated the high speed response of the Aerostatic Seal to significant radial transients. The rotor excursions are in excess of that expected in steam turbine operation. The response of the seal to high levels of rotor eccentricity not only protects the seal segment labyrinth fins from damage, but it is also able to maintain a mean seal segment clearance that is lower than the rotor eccentricity. At low pressure ratios, the ability of the seal segments to respond to high speed rotor movements is reduced, and the mean clearance that the seal maintains increases.

Upon disassembly of the seal segment after high rotor eccentricity testing, all seal segments showed wear on the contact face. As the seal will be expected to operate without maintenance for many years, this is undesirable. Hard facing materials are a possible solution to prevent wear on the contact face. As the material used to manufacture the seal segments used in these tests is not representative of steam turbine grade material, further investigation is left for testing in a steam environment.

The leakage mass flow rate assessment has shown that the Aerostatic Seal is able to reduce leakage over a similar labyrinth seal. Further improvements to the leakage performance of the Aerostatic Seal are possible by optimising the design of the seal segments for different circumferential positions (e.g. 10 O'clock, 2 O'clock segments etc.), and by reducing the mean operating clearance of the seal. These changes can be implemented by modifying the seal segment geometry, or employing different springs to alter the radial pre load on the seal segments. Further leakage reductions are possible by using steps or castellations on the rotor surface, preventing kinetic energy carry over from one cavity too the next.

The Aerostatic Seal has demonstrated dynamic seal characteristics also reported for the HALO seal and floating ring annular seal [20, 22], two non-contacting dynamic seal concepts. Mariot et al [22] demonstrated that the annular seal was able to track high speed rotor vibrations at 21000 rpm and zero to peak amplitude approximately 0.1 mm. This is more responsive than the expected Aerostatic Seal performance at such rotor speeds and amplitudes; the response of the floating ring annular seal is helped by the low coefficient of friction between the carbon ring and the steel seal housing. As previously mentioned it is desirable for the Aerostatic Seal not to respond to small rotor vibrations to prevent wear. The HALO seal has shown a greater reduction in leakage that the Aerostatic Seal described in these tests, 50% or more for the HALO seal at pressure ratios $PR < 3.0$ compared to the Aerostatic Seal at 30-35%. The leakage reductions possible with the HALO seal are dramatic, however the seal appears more complex to manufacture whereas the Aerostatic Seal is designed around existing steam turbine gland construction. The Aerostatic Seal described in this paper was a proof of concept design and not an attempt to find the maximum leakage reduction possible and the authors believe that further leakage reductions are possible with revised designs.

The Aerostatic Seal concept has matured enough to begin testing in a steam environment and is the obvious next step for this technology. High steam temperatures and the use of realistic steam turbine materials will alter the level of friction between the seal segments and the seal holder. It has previously been shown that the level of friction affects Aerostatic Seal performance [3] and designs which are robust to variations in friction level are under consideration.

CONCLUSIONS

This paper describes the demonstration of the Aerostatic Seal, a dynamic clearance seal in a rotating test rig. The seal is a development of the retractable seal design which is widely used in steam turbines.

A new rotating seals rig was commissioned specifically to test the Aerostatic Seal in a rotating environment. The rig used an eccentric rotor to simulate high speed radial rotor excursions, and had inductive sensors to track the position of the seal segments during the tests.

An exhaustive experimental campaign has been conducted at two rotor eccentricity settings, and at a range of pressure ratios and rotor speeds. Tests conducted with a low level of rotor eccentricity showed that operation of the seal was similar to the retractable seal. Seal operation was as expected from previous tests conducted in a non-rotating facility [3]. The seal response was dependant on the circumferential position of the seal segment.

Tests conducted with a high level of rotor eccentricity showed that the seal was able to maintain a mean clearance that was smaller than the level of rotor eccentricity over the full range of rotor speeds tested. A typical labyrinth seal or retractable seal is unable to do this. Furthermore the leakage performance was measured and compared to a comparable segmented labyrinth seal by fixing the seal segments in place. This showed a potential leakage reduction of 35% at the design pressure ratio $PR = 1.5$.

ACKNOWLEDGMENT

This work was supported by the Engineering and Physical Sciences Research Council [grant number EP/K02115X/1]; and GE Power, Steam Power Systems.

REFERENCES

[1] Seaton, J., 2016. Sealing system. European Patent No. EP3002487 A1.

[2] Messenger, A., Williams, R., Ingram, G., Hogg, S., Tibos, S., and Seaton, J., 2015. "A dynamic clearance seal for steam turbine application". In ASME Turbo Expo 2015: Turbine Technical Conference and Exposition, American Society of Mechanical Engineers. Paper No.: GT2015-43471.

[3] Messenger, A., Williams, R., Ingram, G., Hogg, S., Tibos, S., Seaton, J., and Charnley, B., 2016. "Experimental and numerical development of a dynamic clearance seal for steam turbine application". In ASME Turbo Expo 2016: Turbine Technical Conference and Exposition, American Society of Mechanical Engineers. Paper No.: GT2016-56995.

[4] Sneck, H., 1974. "Labyrinth seal literature survey". *Journal of Lubrication Technology,* ***96***(4), pp. 579–581.

[5] Chupp, R. E., Hendricks, R. C., Lattime, S. B., and Steinetz, B. M., 2006. "Sealing in turbomachinery". *Journal of Propulsion and Power,* ***22***(2), pp. 313–349.

[6] Childs, D. W., 1993. *Turbomachinery rotordynamics: phenomena, modeling, and analysis*. John Wiley & Sons.

[7] Benckert, H., and Wachter, J., 1980. "Flow induced spring coefficients of labyrinth seals for application in rotor dynamics". *NASA. Lewis Res. Center Rotodyn. Instability Probl. in High-Performance Turbomachinery p 189-212(SEE N 80-29706 20-37)*.

[8] Li, Z., Li, J., Yan, X., and Feng, Z., 2011. "Effects of pressure ratio and rotational speed on leakage flow and cavity pressure in the staggered labyrinth seal". *Journal of Engineering for Gas Turbines and Power,* ***133***(11), p. 114503.

[9] Vakili, A. D., Meganathan, A. J., Ayyalasomayajula, S., Hesler, S., and Shuster, L. "Advanced labyrinth seals for steam turbine generators". In ASME Turbo Expo 2006: Power for Land, Sea and Air.

[10] Kuwamura, Y., Matsumoto, K., Uehara, H., Ooyama, H., Tanaka, Y., and Nishimoto, S., 2013. "Development of new high-performance labyrinth seal using aerodynamic approach". In ASME Turbo Expo 2013: Turbine Technical Conference and Exposition, American Society of Mechanical Engineers. Paper No.: GT2013-94106.

[11] Gamal, A. J., and Vance, J. M., 2008. "Labyrinth seal leakage tests: tooth profile, tooth thickness, and eccentricity effects". *Journal of Engineering for Gas Turbines and Power,* ***130***(1), p. 012510.

[12] Curtis, E. M., Denton, J. D., Longley, J. P., and Rosic, B., 2009. "Controlling tip leakage flow over a shrouded turbine rotor using an air-curtain". In ASME Turbo Expo 2009: Power for Land, Sea, and Air, American Society of Mechanical Engineers, pp. 885–894. Paper No. GT2009-59411.

[13] Hogg, S. I., and Ruiz, I. G. "Fluidic jet barriers for sealing applications". In ASME 2011 Turbo Expo: Turbine Technical Conference and Exposition, American Society of Mechanical Engineers, pp. 779–788. Paper No. GT2011-45353.

[14] Brandon, R. E., 1984. Segmented labyrinth-type shaft sealing system for fluid turbines. US Patent 4,436,311.

[15] Ferguson, J., 1988. "Brushes as high performance gas turbine seals.". *American Society of Mechanical Engineers, New York*. ASME paper 88-GT-182.

[16] Dinc, S., Demiroglu, M., Turnquist, N., Mortzheim, J., Goetze, G., Maupin, J., Hopkins, J., Wolfe, C., and Florin, M., 2002. "Fundamental design issues of brush seals for industrial applications". *Journal of Turbomachinery,* ***124***(2), pp. 293–300.

[17] Raben, M., Friedrichs, J., and Flegler, J., 2017. "Brush seal frictional heat generation - test rig design and validation under steam environment". *Journal of Engineering for Gas Turbines and Power,* ***139***(3), p. 032502.

[18] Bidkar, R. A., Sevincer, E., Wang, J., Thatte, A. M., Mann, A., Peter, M., Musgrove, G., Allison, T., and Moore, J., 2017. "Low-leakage shaft-end seals for utility-scale supercritical CO2 turboexpanders". *Journal of Engineering for Gas Turbines and Power,* ***139***(2), p. 022503.

[19] Justak, J. F., and Doux, C., 2009. "Self-acting clearance control for turbine blade outer air seals". In ASME Turbo Expo 2009: Power for Land, Sea, and Air, American Society of Mechanical Engineers, pp. 1229–1237. Paper No. GT2009-59683.

[20] San Andrés, L., and Anderson, A., 2015. "An all-metal compliant seal versus a labyrinth seal: A comparison of gas leakage at high temperatures". *Journal of Engineering for Gas Turbines and Power,* ***137***(5), p. 052504.

[21] Arghir, M., Nguyen, M.-H., Tonon, D., and Dehouve, J., 2012. "Analytic modeling of floating ring annular seals". *Journal of Engineering for Gas Turbines and Power,* ***134***(5), p. 052507.

[22] Mariot, A., Arghir, M., Hélies, P., and Dehouve, J., 2016. "Experimental analysis of floating ring annular seals and comparisons with theoretical predictions". *Journal of Engineering for Gas Turbines and Power,* ***138***(4), p. 042503.

[23] Waschka, W., Wittig, S., and Kim, S., 1992. "Influence of high rotational speeds on the heat transfer and discharge coefficients in labyrinth seals". *Journal of turbomachinery,* ***114***(2), pp. 462–468.

[24] Hodkinson, B., 1939. "Estimation of the leakage through a labyrinth gland". *Proceedings of the Institution of Mechanical Engineers,* ***141***(1), pp. 283–288.

[25] Martin, H. M., 1908. "Labyrinth packings". *Engineering,* ***85***(10), pp. 35–38.

[26] Gurevich, M. I., 1965. *The theory of jets in an ideal fluid*. Academic Press.

[27] Eser, D., and Kazakia, J. Y., 1995. "Air flow in cavities of labyrinth seals". *International Journal of Engineering Science,* ***Vol. 33***(15), pp. 2309–2326.